THE JOURNAL OF COMPARATIVE NEUROLOGY 452:11–23 (2002)

Central Projections of the Utricular Nerve in the Gerbil

SHAWN D. NEWLANDS,[1] IAN M. PURCELL,[1,2] GOLDA ANNE KEVETTER,[1,2] AND ADRIAN A. PERACHIO[1,2,3]

[1]Department of Otolaryngology, University of Texas Medical Branch, Galveston, Texas 77555

[2]Department of Anatomy & Neurosciences, University of Texas Medical Branch, Galveston, Texas 77555

[3]Department of Physiology & Biophysics, University of Texas Medical Branch, Galveston, Texas 77555

ABSTRACT

The central projections of primary afferent fibers in the utricular nerve, which convey linear head acceleration signals to neurons in the brainstem and cerebellum, are not completely defined. The purpose of this investigation was twofold: 1) to define the central projections of the gerbil utricular afferents by injecting horseradish peroxidase (HRP) and biotinylated dextran amine (BDA) into the utricular macula; and 2) to investigate the projections of individual utricular afferents by injecting HRP intracellularly into functionally identified utricular neurons. We found that utricular afferents in the gerbil projected to all divisions of the vestibular nuclear complex, except the dorsal lateral vestibular nucleus. In addition, terminals were observed in the interstitial nucleus of the eighth nerve, nucleus Y, external cuneate nucleus, and lobules I, IV, V, IX, and X of the cerebellar vermis. No projections appeared in the flocculus or paraflocculus. Fibers traversed the medial and intermediate cerebellar nuclei, but terminals appeared only occasionally. Individual utricular afferents collateralize extensively, projecting to much of the brainstem area innervated by the whole of the utricular nerve. This study did not produce complete filling of individual afferent collateral projections into the cerebellar cortex. J. Comp. Neurol. 452:11–23, 2002.

Indexing terms: vestibular nuclei; cerebellar nuclei; vermis; biotinylated dextran amine; nucleus Y; horseradish peroxidase

A variety of sensory systems register information about our relative position as we move through space; control of our balance and locomotion depends on information originating in the vestibular periphery. Primary vestibular afferents, which innervate the bilateral otolith (utricular and saccular) maculae, sense gravitational and translational accelerations and thus help control a variety of motor and visceral systems. Recent literature has highlighted the difficulty in understanding how the brain discriminates afferent signals arising from changes in head position relative to gravity from signals due to translational motion (Angelaki et al., 1999; Merfield et al., 1999). This discrimination is critical, as the kinematic demands on the oculomotor and postural systems are different for tilt vs. translation. However, the dynamic responses of utricular afferent neurons stimulated by either tilt or translational motion are indistinguishable. Because afferents originate in relatively discrete areas of the utricular macula (Fernández et al., 1990), the response of individual afferent neurons is determined by the sensitivity to deflection of hair cells in that area (Goldberg et al., 1990). Central neurons related to the otolith organs show more complex behavior in response to gravitational, inertial, and rotational stimulation (Angelaki and Dickman, 2000) than do peripheral otolith afferents, presumably because

Grant sponsor: National Institute of Health; Grant numbers: R01-DC00385 and K08-DC00182.

*Correspondence to: Adrian A. Perachio. Ph.D., University of Texas Medical Branch, Department of Otolaryngology, 301 University Boulevard, 7.102 Medical Research Building, Galveston, TX 77555-1063.
E-mail: aperachi@utmb.edu

Received 24 July 2001; Revised 16 May 2002; Accepted 13 June 2002

DOI 10.1002/cne.10350

Published online the week of August 19, 2002 in Wiley InterScience (www.interscience.wiley.com).

inputs from the periphery converge (otolith-otolith and canal-otolith convergence).

An understanding of the anatomic properties of the central otolith system is essential for understanding these and other critical issues in the processing of otolith signals. Elegant morphophysiological studies (Goldberg et al., 1990) have provided data on the peripheral projections to the sensory epithelia of the labyrinth, but central projections of vestibular primary afferents have not been as well described.

The projections of vestibular afferents from the vestibular organs to the major vestibular nuclei have long been recognized. Those pathways have been demonstrated in a number of mammalian species, with a variety of tracing techniques. Early studies initially characterized the projection of the vestibular nerve to the vestibular nuclei using the Golgi method (Ramon y Cajal, 1909; Lorente de No, 1933). Others used silver impregnation techniques to trace degeneration of afferents after vestibular nerve lesions (Stein and Carpenter, 1967; Brodal and Høivik, 1964; Gacek, 1969; Carpenter et al., 1972; Korte, 1979; Korte and Mugnaini, 1979). These studies lacked the precision available with current techniques. More recently, investigators have used either anterograde or retrograde neuronal tracer techniques to look at projections from the entire nerve (Carleton and Carpenter, 1984; Carpenter and Cowie, 1985; Burian et al., 1990; Newman et al., 1992). Whereas many anatomical studies treated the vestibular nerve as a whole, others revealed projections of the vestibular afferent nerve from specific end organs (Siegborn and Grant, 1983; Kevetter and Perachio, 1986; Fredrickson and Trune, 1986; Didier et al., 1987; Siegborn et al., 1991; Gstoettner et al., 1992; Imagawa et al., 1995; Naito et al., 1995; Dickman and Fang, 1996). Still other studies have used intracellular neural tracers to label characterized primary afferent fibers (Mannen et al., 1982; Perachio et al., 1988; Sato et al., 1989; Sato and Sasaki, 1993; Imagawa et al., 1995, 1998).

That body of work has consistently found that vestibular afferents project to all the major ipsilateral vestibular nuclei, with the possible exception of the dorsal division of the lateral vestibular nucleus (LVe). Not all the accessory vestibular areas receive primary afferent input. Primary afferents innervate nucleus Y (Fredrickson and Trune, 1986; Kevetter and Perachio, 1986; Didier et al., 1987), but not cell groups X, F, and Z (Burian et al., 1990). The interstitial nucleus of the vestibular nerve (I8) receives heavy afferent input. The ipsilateral vermal lobules of the cerebellum, particularly lobules IXd and X, also receive input from canal and otolith primary afferents (Gerrits et al., 1989; Barmack et al., 1993; Purcell and Perachio, 2001), whereas the flocculus receives less input, which is derived from the ampullary nerves (Purcell and Perachio, 2001). Similarly, studies using horseradish peroxidase (HRP) or autoradiographic techniques (Carleton and Carpenter, 1984; Gerrits et al., 1989) have not reliably replicated earlier findings of primary afferent innervation of the cerebellar nuclei, particularly the medial and lateral cerebellar nuclei (Brodal and Høivik, 1964). The medullary reticular formation also receives some vestibular sensory input (Korte, 1979; Carleton and Carpenter 1984; Imagawa et al., 1995).

The current experiments investigate the central projections of gerbil utricular afferents. The central projections of saccular, posterior canal, and horizontal canal afferents in the gerbil previously reported by Kevetter and Perachio (1986; Perachio et al., 1988) offer a contrast to the innervation pattern from the utricular macula. In this study, the results of injecting biotinylated dextran amine (BDA) or HRP directly into the sensory neuroepithelium of the utricular macula or by filling individual utricular afferents with HRP are compared with the distribution of projections from the other end organs previously studied. The specificity of the end organ injections was controlled by direct microscopic examination of all the end organs.

Abbreviations

6	abducens nucleus
12	hypoglossal nucleus
4V	4th ventricle
7n	facial nerve
8n	vestibulocochlear nerve
ant	anterior
AP	area postrema
BDA	biotinylated dextran amine
CB1	cerebellar lobule I
CB2	cerebellar lobule II
CB8	cerebellar lobule VIII
CB9	cerebellar lobule IX
CB10	cerebellar lobule X
Cu	cuneate nucleus
d	dorsal
DC	dorsal cochlear nucleus
DPGi	dorsal paragigantocellular nucleus
ECu	external cuneate nucleus
Fl	flocculus
FVe	F cell group of the vestibular complex
g7	genu of the facial nerve
GC	granular cell layer
Gr	gracile nucleus
HRP	horseradish peroxidase
I8	interstitial nucleus of the eighth nerve
icp	inferior cerebellar peduncle
Inf	infracerebellar nucleus
IntA	interposed cerebellar nucleus, anterior
IntP	interposed cerebellar nucleus, posterior
IntPPC	interposed cerebellar nucleus, posterior parvicellular part
lat	lateral
Lat	lateral (dentate) cerebellar nucleus
LatPC	lateral cerebellar nucleus, parvicellular part
LVe	lateral vestibular nucleus
Me5	mesencephalic trigeminal nucleus
Med	medial (fastigial) cerebellar nucleus
mlf	medial longitudinal fasciculus
MVe	medial vestibular nucleus
MVeMC	medial vestibular nucleus, magnocellular
MVePC	medial vestibular nucleus, parvicellular
PC	Purkinje cell layer
PCRt	parvicellular reticular nucleus
PFl	paraflocculus
Pr	prepositus nucleus
PSol	parasolitary nucleus
py	pyramidal tract
Ro	nucleus of Roller
SolDM	nucleus of the solitary tract, dorsomedial part
Sp5I	spinal trigeminal nucleus, interpolar part
SpVe	spinal vestibular nucelus
SuVe	superior vestibular nucleus
VeCb	vestibulocerebellar nucleus
VNC	vestibular nuclear complex
X	cell group X
Y	nucleus Y
Z	cell group Z

These findings have been described in part in previous preliminary reports (Perachio et al., 1984; Perachio and Kevetter, 1986a,b).

MATERIALS AND METHODS

Surgical procedures

Experiments were performed on young adult Mongolian gerbils of either gender weighing 70–100 g. We performed all procedures according to the National Institutes of Health *Guide for the Care and Use of Animals in Research*, and the research protocol was reviewed and approved by the University of Texas Medical Branch's Animal Care and Use Committee. We initially anesthetized the animals with sodium pentobarbital (40 mg/kg i.p.) and supplemented with ketamine hydrochloride (20 mg/kg i.m.) as needed. A thermal pad maintained normal body temperature. For the intracellular labeling experiments, we placed the animals in a stereotaxic device, made a midline scalp incision, exposed the surface of the cerebellum, and lowered electrodes through the cerebellum into the vestibular nerve for recording and intracellular labeling of neurons. The scalp incision was closed and the animals recovered.

For the macular injection experiments, we opened the bulla and drilled through the exposed bony labyrinth with a small dental burr to visualize the utricular macula. After injection of the macula, the bony labyrinth was resealed with bone wax. The scalp incision was closed and the animals recovered.

Animals in both groups were sacrificed for histologic examination after appropriate recovery times. A lethal injection of sodium pentobarbital (50 mg in 1 ml of water) was given intrahepatically. The animal was perfused through the left ventricle with saline followed by the appropriate fixative.

Single-unit injections

Micropipettes, containing 10% HRP (type VI; Sigma, St. Louis, MO) in 0.5 M KCl and 0.05 M Tris buffer (pH 7.4), were stereotaxically directed into the postganglionic vestibular nerve. DC membrane resting potentials of at least −30 mV, overshooting action potentials, and sensitivity to hyper- or depolarizing currents of <1.0 nA indicated intracellular penetrations. HRP was injected into the axon by passing a sinusoidal current (2.5 Hz, 10–15 nA peak to peak current with a 30% peak to peak current positive DC offset). Successful labeling usually required injection durations of more than 6 minutes. The majority of intracellularly injected neurons responded characteristically to pitch and yaw rotations and to static tilt on a gimbal-mounted platform (Perachio and Correia, 1983). We assumed that neurons sensitive to ipsilateral yaw were related to the lateral canal, neurons sensitive to nose-down dynamic tilt were related to the anterior canal, and neurons sensitive to nose-up dynamic tilt were related to the posterior canal. Only neurons sensitive to static tilt were included in this study. A few neurons were tested and injected while on a linear sled. In these cases, we injected only neurons sensitive to horizontal translation. We presumed that visualization of the labeled cell body in the superior vestibular ganglion corroborated a utricular origin of the labeled cells. Furthermore, in most cases, the labeled peripheral axonal process could be traced into the utricular nerve.

In most animals, we made injections into the vestibular nerve on both sides. In several animals, we injected more than one neuron on a side. When more than one cell was injected per side, we used the data only if all of the injected cells were sensitive to static tilt or linear translation and all the cell bodies were located in the superior ganglion.

Macular injections

After exposure of the end organ (as discussed above) we injected one of two tracers directly into one to three areas of the sensory epithelium of the utricular macula. We injected HRP (10–20% Sigma type VI, or 30% Miles [Elkhart, IN] in 0.5 M KCl and 0.15 M Tris buffer, pH 7.4) through micropipettes (tip diameter 3–10 μm) using iontophoresis (15-second-duration pulses of 3–10 μA positive current at a 50% duty cycle for 3–10 minutes). Alternatively, BDA (3000 MW [Molecular Probes, Eugene, OR] 10% in 0.1 M phosphate buffer, pH 7.4) was injected iontophoretically through micropipettes (tip diameter 30–50 μm) using DC of 5 μA for 5 minutes.

Histologic processing

Animals injected with HRP survived for 24–48 hours, whereas those injected with BDA survived for 144–240 hours. Gerbils that received HRP injections were perfused transcardially with physiologic saline containing 10,000 U/liter of heparin, followed by 1% paraformaldehyde, 1.25% glutaraldehyde in 0.1 M phosphate buffer, pH 7.4. The same aldehyde solution with the addition of 25% sucrose was used for a final flush. Gerbils injected with BDA were perfused with warm physiologic saline with heparin (10,000 U/liter) followed by cold 4% paraformaldehyde, 0.1 M L-lysine, and 0.01 M sodium-m-periodate in 0.1 M phosphate-buffered saline (Veenman et al., 1992).

We handled the labyrinth sensory organ tissues in one of three ways. In the intracellular HRP experiments done on the tilt platform, the labyrinth was dissected and left attached to the brainstem. The tissue was then decalcified for 2 weeks in a solution of 0.1 M EDTA (Kiang et al., 1982). In the animals with HRP injected into the utricular macula, the entire temporal bone was left attached to the brainstem and decalcified in EDTA for 2–3 weeks prior to processing. For animals in which we intracellularly filled axons with HRP on the linear track and those in which we had injected BDA into the utricular macula, we individually harvested the end organs (two otolith macula and three semicircular canal cristae). The tissue was then dehydrated, embedded in EPON 812, and examined as described previously (Purcell and Perachio, 1997; Purcell and Perachio, 2001).

We sectioned the brainstem tissue in horizontal, coronal, or parasagittal planes. Those cut in the horizontal plane included all single-unit HRP fill experiments, four HRP macular injections, and one BDA macular injection. Those cut in the coronal plane included four HRP macular injections and one BDA macular injection. The tissue cut in the parasagittal plane included two HRP macular injections and three BDA macular injections. The individual end organs were processed as whole mounts after the pigmented epithelium and membranous labyrinth were dissected from the sensory neuroepithelium. HRP tissue was processed directly using a cobalt-intensified diaminobenzidine/glucose oxidase reaction (Kevetter and Perachio, 1986). BDA tissue was processed by incubation in 1:100 avidin-biotin (Vector, Burlingame, CA) and 0.25%

(central tissue) or 0.5% (peripheral tissue) Triton-X 100 for 2.5 hours (Purcell and Perachio, 1997). A cobalt-intensified diaminobenzidine/glucose oxidase reaction (Kevetter and Perachio, 1986) was then used to demonstrate the BDA labeling. Sections were viewed with brightfield microscopy. Decalcification prior to the HRP or BDA reaction preserved the integrity of the inner ear and vestibular nerve so that the specificity of the injection sites could be verified.

For peripheral injections, we analyzed only samples without spread of label to adjacent end organs. As previously reported, anterograde transganglionic transport of HRP occurs after iontophoretic injection of the enzyme into vestibular end organs in the gerbil (Kevetter and Perachio, 1986). Spillage of HRP into the endolymphatic or perilymphatic spaces does not result in transganglionic transport or labeling of ganglion cells (Lee et al., 1992). Therefore, we considered injections to be specific in the absence of spread of tracer to adjacent sites. All identification of anatomic structures is based on the atlas of Paxinos and Watson (1998). Images were captured using a Coolsnap fx camera (Roper Scientific, Trenton, NJ) and MetaMorph software (Universal Imaging Corporation, Downington, PA). Brightness, contrast, uneven illumination, and sharpness were adjusted in captured images using Adobe Photoshop software (version 5.0; Adobe Systems, Mountain View, CA) when deemed necessary (Saper, 1999).

RESULTS

Macular injections

Useful information was obtained from nine gerbils in which one utricular macula was injected with HRP and from five that were injected with BDA. Tissue sections from the horizontal, transverse, or parasagittal cardinal head planes facilitated examination of specific aspects of the projections. Horizontal sections best displayed the anterior/posterior and medial/lateral courses of the nerve, wheras parasagittal sections showed best the projections to the cerebellar lobules.

Injection specificity

Within the macula, the injection sites appeared as a lesion usually centered in the striolar region. All the injections were subtotal; the primary concern was avoidance of label spread beyond the macula. Dense labeling of afferent fibers and terminals appeared around the lesion (Fig. 1A). In HRP-labeled material, no reaction product was observed in the other sensory neuroepithelia. BDA injections occasionally labeled fine fiber processes in ipsilateral sensory end organs, terminating exclusively in small bouton-like endings that were identical in appearance and distribution to those following anterograde labeling of vestibular efferent neurons (Purcell and Perachio, 1997). These efferent neuron terminals are collateral projections to other end organs that transported label from the utricular injection site; this is not a result of spillage of tracer from the injection. Bilateral retrograde labeling of vestibular efferent cell bodies appeared in all cases.

Central projections of utricular afferents

Vestibular nerve. The processes and cell bodies of neurons within the superior division of the vestibular

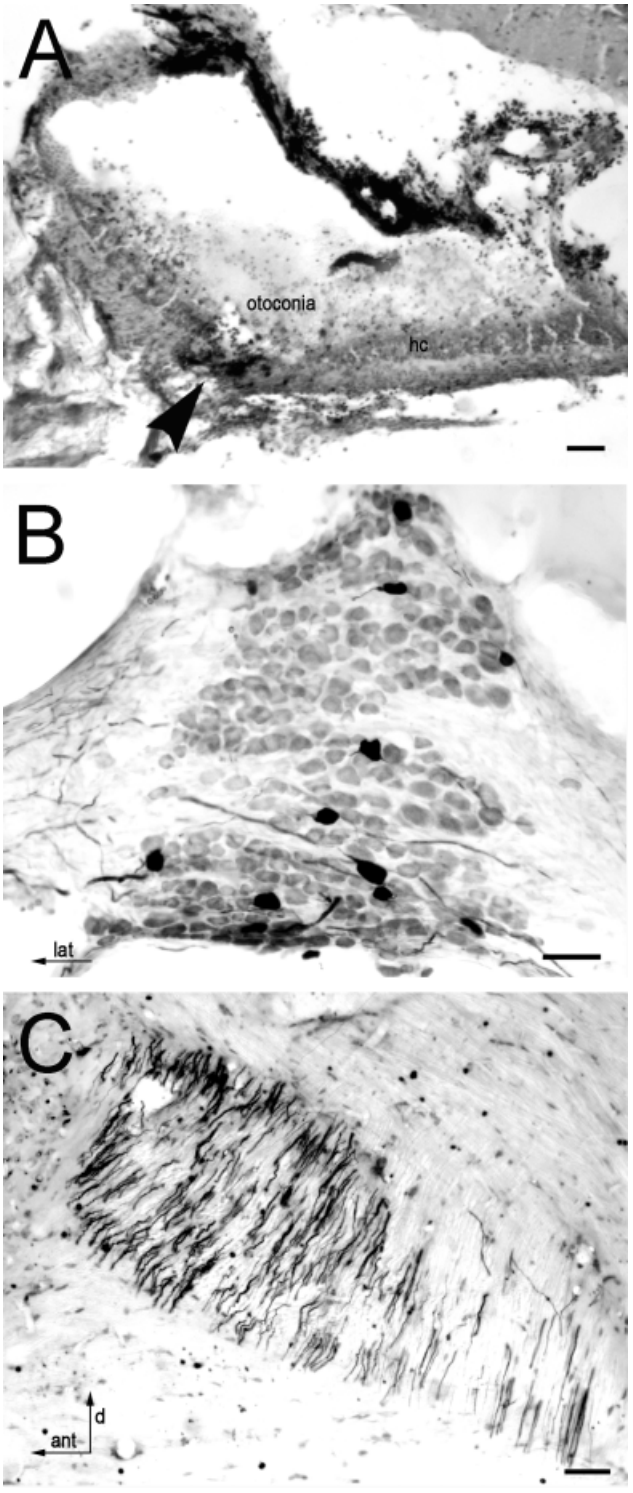

Fig. 1. **A:** Injection site in the utricular macula. Arrowhead marks HRP labeling confined to a small area of the utricular macula. **B:** A horizontal section through the superior division of the vestibular ganglion demonstrating several labeled cell bodies. No labeled cell bodies were seen in the inferior division of the ganglion. **C:** A parasagittal section through the vestibular nerve. The majority of the labeled fibers are in the anterior portion of the nerve. Scale bar = 100 μm in A; 50 μm in B,C.

ganglion were labeled by anterograde transganglionic transport of both HRP and BDA (Fig. 1B). The labeled cell bodies in the superior division of the vestibular ganglion were not organized in any apparent topographical manner. The cells were bipolar. There was no evidence of axonal branching within the ganglion of either the peripheral or central axon. Typically, the peripheral fiber was thinner than the diameter of the central axon (Perachio et al., 1984). The central projecting axons emerged from the ganglion in a bundle of parallel fibers coursing in the rostral portion of the nerve root (Fig. 1C).

In general, BDA injections produced labeling over greater distances and more extensive labeling of bouton terminations of the central axons. The fibers traveled lateral to medial under the dorsal cochlear nucleus and remained in the anterior half of the vestibular nerve. Within the vestibular nerve, a portion of the fibers gave off short collaterals that ramified into terminal branches, ending in bouton-like profiles among the cells of I8 (Fig. 2C). The fiber bundle traveled medially, in a caudal and dorsal course along the lateral margin of the restiform body. Immediately lateral to the border of the ventral LVe, all the axons appeared to branch in the horizontal plane at nearly a right angle into an ascending and descending portion. The descending portion coursed in bundles of parallel fibers lateral to the spinal vestibular nucleus (SpVe) along the length of the vestibular nuclear complex (VNC) in a posterior and slightly medial direction (see Fig. 3B).

These fibers generally could not be traced past the external cuneate nucleus (ECu); however, occasionally a fiber was seen in the gracilis nucleus. Collaterals from the descending fibers (which were best seen on horizontal sections) branched medially at right angles to the projection pathway toward the parvicellular (MVePC) and magnocellular (MVeMC) divisions of the MVe and the SpVe (see Fig. 3B). The ascending branches coursed dorsally lateral to the LVe and through the lateral portion of the superior vestibular nucleus (SuVe) into the cerebellum. Here, the fibers fanned out and passed through the anterior interposed cerebellar (IntA) and medial cerebellar (Med) nuclei as they passed medially and posteriorly toward the vermis.

Projections to the vestibular nuclei. Utricular afferents projected to all the major vestibular nuclei (see Fig. 4). The heaviest concentration of labeling was in the lateral and rostral SuVe, rostral MVePC, and MVeMC (see Fig. 3A,C). The dorsal LVe was almost unlabeled, although fibers coursing toward the cerebellum appeared in the lateral portions of the nucleus, and labeling was noted in the ventral LVe (see Fig. 3A). In the MVePC, labeling was dense in the entire rostral quarter of the nucleus but was concentrated laterally and ventrally in a more caudal area. Except in the rostral pole, the lateral-ventral region of the nucleus was very sparsely labeled. Fibers coursed through and along the SpVe as mentioned above, but the amount of terminal labeling seen was less than that in the MVePC and SuVe. The labeling in the SpVe was heaviest in the lateral, caudal portion of the nucleus. MVeMC labeling was less dense than in the MVePC (see Fig. 3A). Labeling of the caudal nucleus Y was lateral to the LVe at a level caudal to the SuVe (Fig. 2B). Moving rostrally, nucleus Y labeling was lateral to the SuVe and dorsal to the inferior cerebellar peduncle (Fredrickson and Trune, 1986). Labeling was seen as far lateral as the lateral

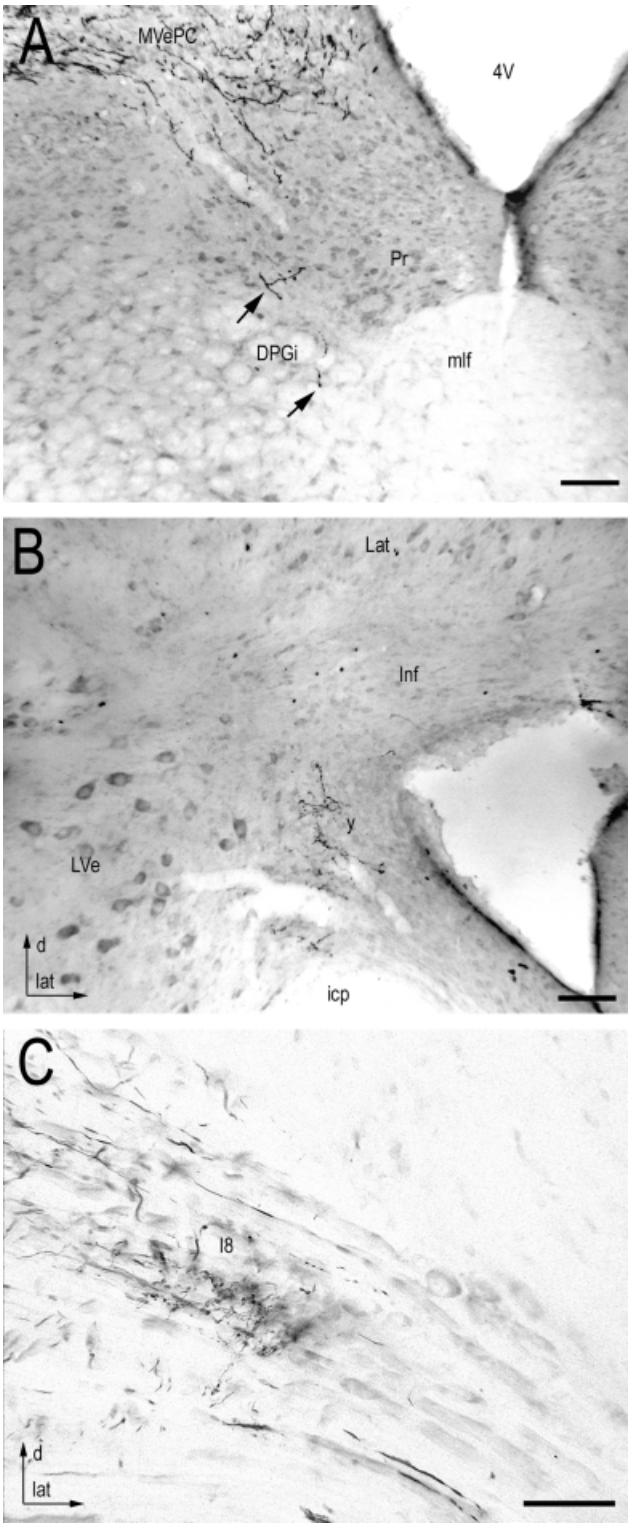

Fig. 2. **A:** BDA labeled fiber projecting ventromedially into the dorsal paragigantocellular nucleus of the reticular formation. Horizontal section. Bouton endings are seen (lower arrowhead). **B:** Nucleus Y viewed in horizontal section with multiple en passant and spray bouton endings. **C:** Interstitial nucleus of the eighth nerve following BDA injection into the utricular macula. Horizontal section. Scale bar = 50 μm.

recess of the fourth ventricle. This labeling involved the infracerebellar nucleus (Inf), which can be distinguished from Y by the presence of fibers running between the neuronal soma (Gacek 1977; Fredrickson and Trune, 1986). Labeling of Y was denser than in the infracerebellar nucleus. The Y labeling was less than was seen with sacculus injection (Kevetter and Perachio, 1986).

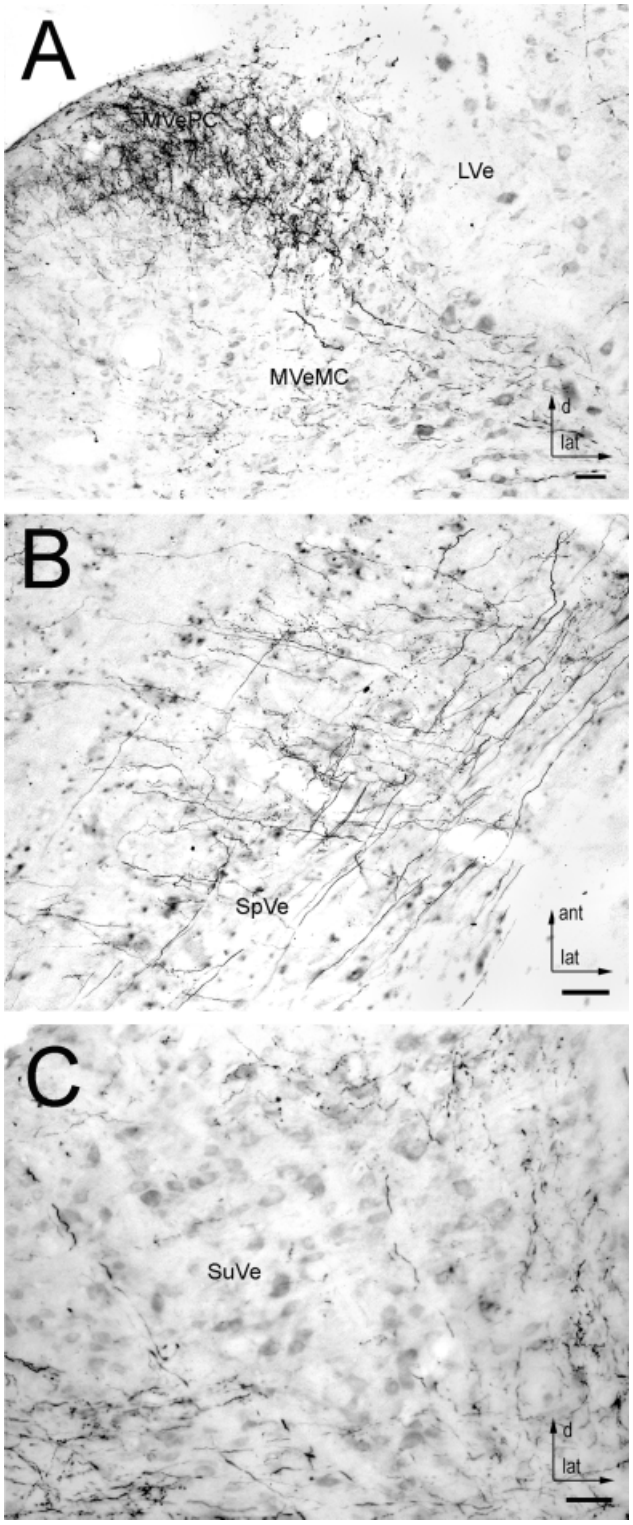

Extravestibular projections. Extravestibular brainstem labeling was sparse. The majority of descending fibers terminated at the level of the ECu where BDA labeling, but not HRP injections, revealed terminals in the nucleus. Fibers were also seen, at least on occasion, in the nucleus gracilis, the spinal nucleus of the trigeminal nerve, the dorsal paragigantocellular reticular nucleus (DMGi; Fig. 2A), the parasolitary nucleus, the ventrolateral reticular formation, and the nucleus of Roller. At the caudal end of the MVe, labeling appeared in the dorsomedial part of the solitary nucleus and the medial aspect of the cuneate nucleus in the best-labeled specimens (Fig. 4). Careful examination of the ipsilateral nucleus of the sixth nerve failed to reveal any terminals or projections. Fibers that originated from the e-group and terminated in the periphery were seen to cross at the level of this nucleus (Perachio and Kevetter 1989). In the rare case in which fibers appeared in the prepositus nucleus (Pr), no terminals were observed.

Cerebellar projections. The ascending branch of the nerve sent fibers dorsally through and posterior to the superior cerebellar peduncle. The fibers ascended between the interposed nuclei and through the IntA; however, definitive evidence of termination in this nucleus was not seen. Fibers were occasionally seen in Med along with a rare terminal (Fig. 5B). A rare terminal was also seen in the posterior division of the interposed nucleus (IntP; Fig. 5C). No projections to the flocculus were seen. However, there was significant labeling in midline cerebellar lobules. This labeling was most dense in lobule IX (Fig. 5A) and included fibers in the white matter and in the granular cell layer. Large characteristic mossy fiber terminals were noted in the granular cell layer of dorsal lobule I (Fig. 5E), ventral lobule IX (Fig. 5F), and dorsal lobule X (Fig. 5D). Fibers were also seen in the white matter of lobule IV and V, but no terminals were seen. All the cerebellar projections were very light compared with the VNC terminations, perhaps due to either difficulty in anterograde transport of the tracer distally, a relative sparseness of that projection, or both. The strongest cerebellar projections were to ventral lobule IX and dorsal lobule X.

Single-unit injections

We successfully injected 70 presumed utricular afferents in 47 gerbils. These cells were characteristically sensitive to tilt or translation, had cell bodies located in the superior ganglia (Fig. 6A), and were not sensitive to rotation. Furthermore, no other cells were injected in the same nerve that did not share those characteristics. Central projections could be traced at least as far as the vestibular nuclei for four of five regularly firing afferents, two of

Fig. 3. Vestibular nuclei projections following utricular injection with BDA. **A:** Denser labeling is noted in the MVePC than in the MVeMC. Transverse section. **B:** Fibers descending in the lateral portion of the SpVe send collateral fibers perpendicularly into the medial portion of the nucleus and into the caudal MVePC. Horizontal section. **C:** Ascending fibers traverse the lateral portion of the superior vestibular nucleus in transit to the cerebellum. Labeling is densest in this nucleus in the parvicellular lateral, superior, and anterior portions. Lower right corner demonstrates labeling in the rostral MVePC. Transverse section. Scale bar = 50 μm.

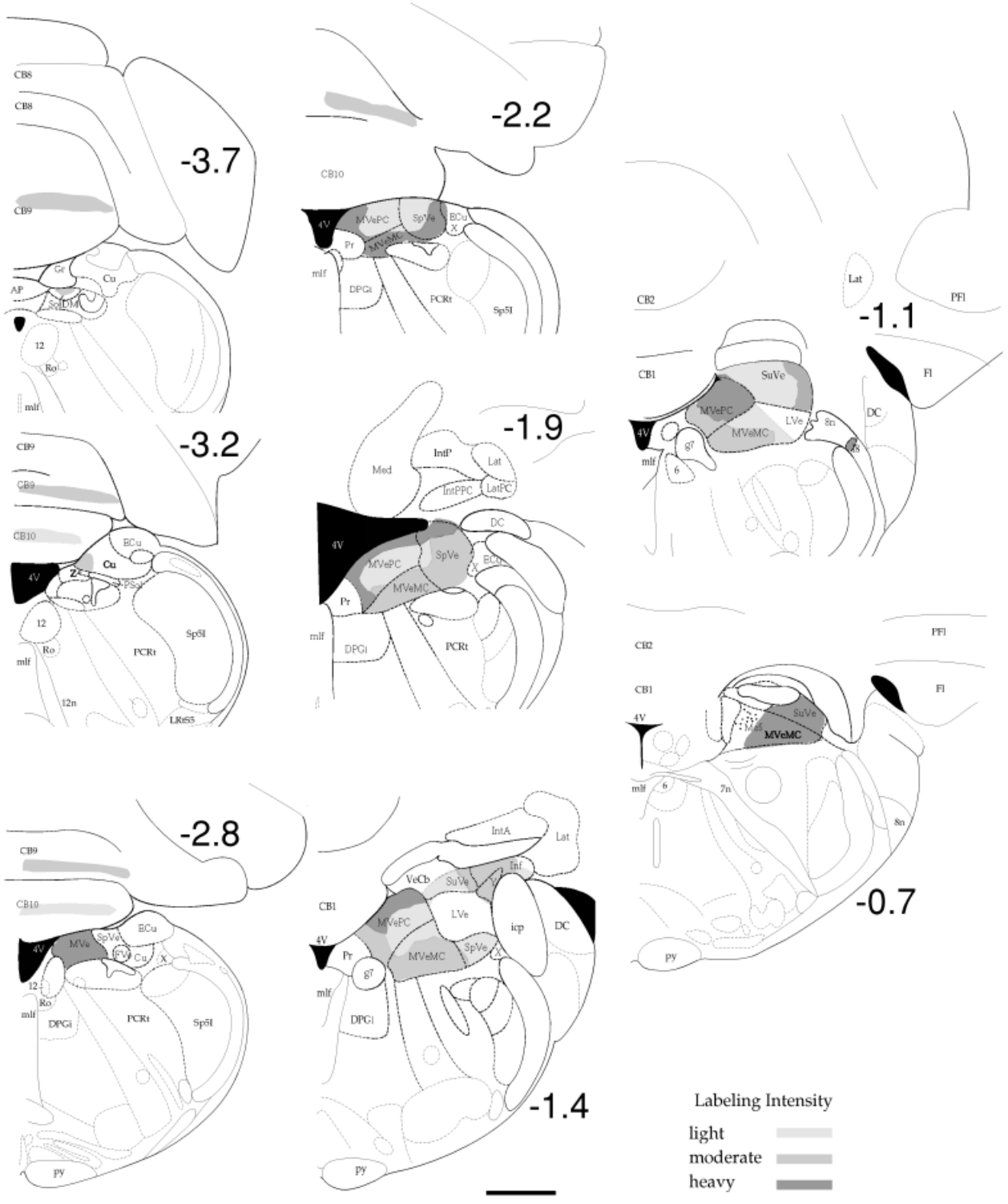

Fig. 4. Schematic representation of terminal field labeling following utricular macula injection in gerbil GA171. Darker shades of gray represent heavier terminal labeling density. Scale bar = 1 mm.

three intermediate firing afferents, and 40 of 63 irregularly firing afferents.

The projections of some well-labeled individual neurons recapitulated the course of the whole nerve, whereas other cells demonstrated stronger projections either of the ascending branch to the SuVe and cerebellum, or the descending branch toward the SpVe. Individual branches into the cerebellar cortex were not seen, although fibers

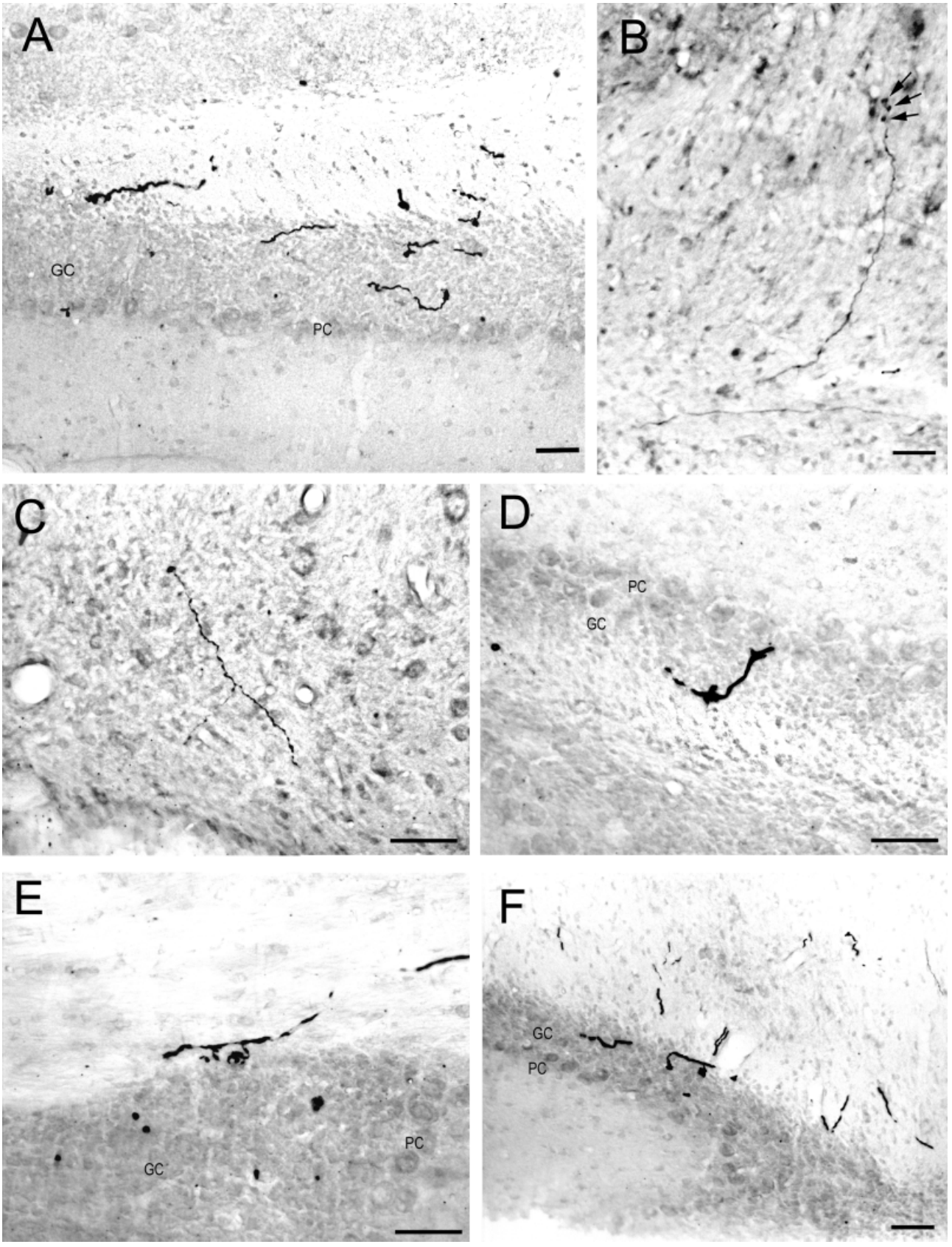

Fig. 5. Cerebellar projections following BDA end organ injection. **A:** Transverse section through the cerebellar lobule IX. Fibers course posteriorly in the white matter of the lobule before terminating in the granular cell layer on the ventral side of the lobule. **B:** Fiber ascending in the medial cerebellar nucleus before terminating in a spray ending. **C:** Multiple en passant boutons in the posterior division of the interposed cerebellar nucleus. **D–F:** Examples of mossy fiber terminals in the granular cell layers in the dorsal side of lobule X (D), lobule I (E), and ventral lobule IX (F). Scale bar = 50 μm.

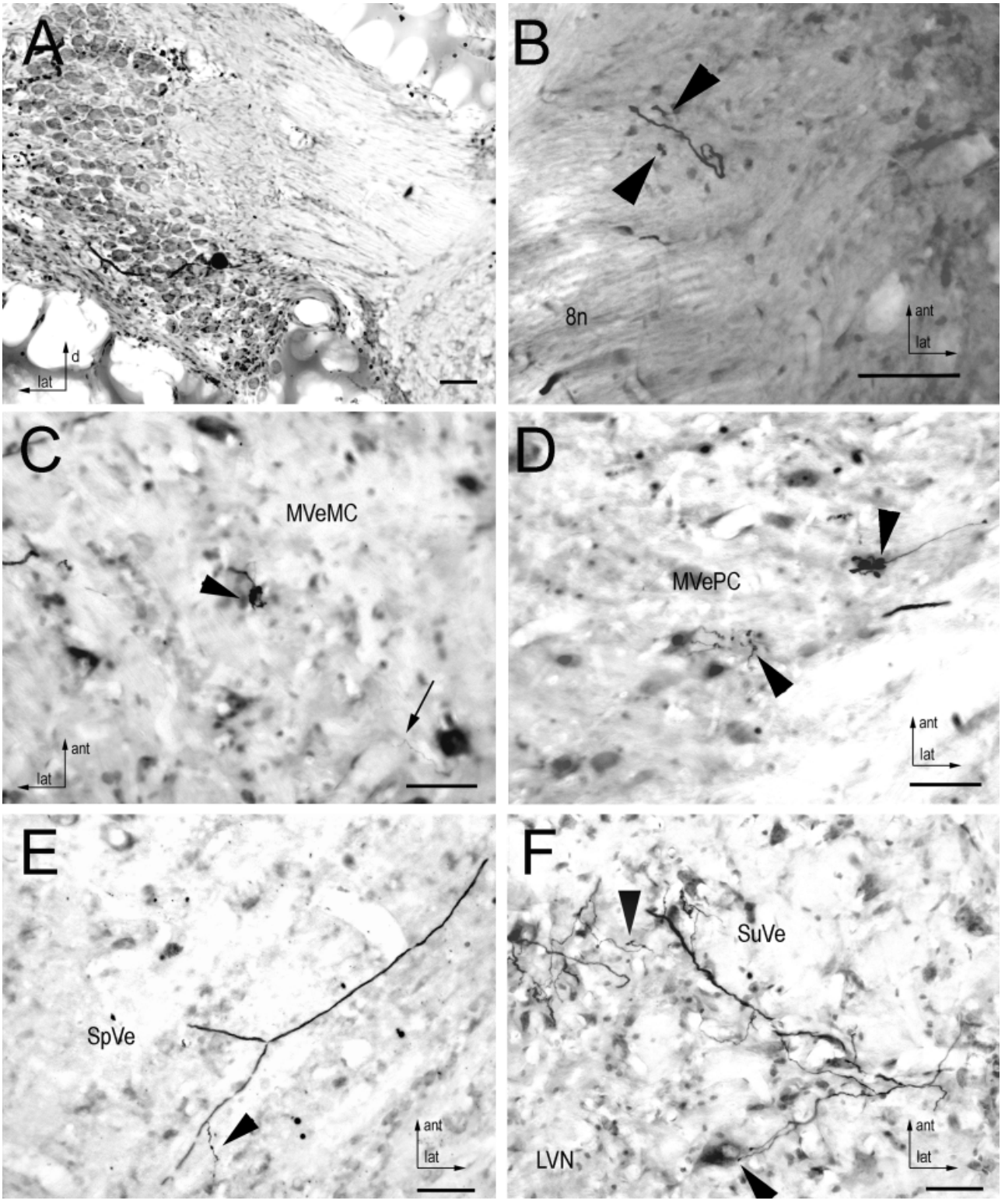

Fig. 6. Labeling following intracellular injection of HRP into single afferents. All are sectioned horizontally. **A:** Filled superior vestibular ganglion cell. **B:** Projection into the interstitial nucleus of the eighth nerve. Arrowheads point to boutons. **C:** Spray bouton endings in the MVeMC indicated by arrowheads. The small arrow points to an additional small fiber with boutons en passant. **D:** Boutons in the MVePC, indicated by arrowheads. **E:** Descending fiber in SpVe with medially directed collateral fibers. Arrowhead points to small collateral with boutons en passant. **F:** Terminal labeling in the SuVe. Arrowheads point to boutons. Each scale bar = 50 μm.

were traced into lobule X, IntA, IntP, and Med. No terminals were seen in these cerebellar nuclei either. In addition, labeled axons of single units did not trace to extravestibular medullary regions. Figure 6 demonstrates projections of individually labeled afferents to I8 and the major vestibular nuclei. The heaviest terminations were again seen in the MVePC (Fig. 6C), especially in rostral and dorsal areas. Terminals were also evident in the MVeMC (Fig. 6D), lateral SuVe (Fig. 6F), and sparsely throughout the SpVe (Fig. 6E). Not every afferent sent a branch to I8, but many did (Fig. 6B). No differences were noted between termination patterns of the irregular versus regular afferents; however, the small numbers of regular units filled make definitive comparisons impossible.

DISCUSSION

Labeling specificity

Previous studies have used a variety of techniques to describe vestibular nerve anatomy in mammals. Siegborn and Grant (1983) and Siegborn et al. (1991) applied anterograde tracers, either HRP or wheat germ agglutinin-HRP, directly to the cut end of isolated anterior canal, posterior canal, utricular, or horizontal canal nerves. They did not confirm histologically the specificity of the application. Gstoettner et al. (1992) placed crystals of HRP on the cut ends of branches of the vestibular nerve in guinea pig. They assessed the posterior ampullary, utricular, saccular, and common horizontal and anterior ampullary nerves individually. To avoid tracer spread, they sealed off the rest of the labyrinth with bone wax. They showed in controlled studies that sealing the cut nerve branches and the labyrinth with bone wax minimized HRP transport to the cerebellum and brainstem, allowing them to assume labeling of one end organ at a time. HRP crystals placed directly on damaged neuroepithelium of an end organ or HRP injected into the labyrinth produce specific labeling (Fredrickson and Trune, 1986; Lee et al., 1992). Undamaged epithelium does not take up HRP. As we did in our study, Kevetter and Perachio (1986) injected HRP directly into the posterior semicircular canal crista or saccular macula without spread to the other end organs. In contrast, Carleton and Carpenter (1984) were unable to effectively and consistently limit the spread of tritiated amino acid tracers injected into specific end organs.

Injection of tracer into a single axon with confirmed peripheral projection produces the most specific labeling of afferents. Although this technique is specific, incomplete filling of the neuron or sampling bias may reduce its sensitivity (Sato and Sasaki, 1993). Specificity of multiunit injections can only be confirmed by inspecting the other end organs. In this study, as in a previous study (Kevetter and Perachio, 1986), we examined each of the other end organs and the vestibular ganglion and found no evidence of spread or uptake of tracers by other end organs. Our findings confirm those of previous studies (Kevetter and Perachio, 1986; Lee et al., 1992) showing that the endolymphatic and perilymphatic spaces do not take up HRP. The same conclusions can be drawn for BDA.

As reported in other studies of canal afferents (Mannen et al., 1982; Perachio et al., 1988; Sato et al., 1989), projections labeled via intra-axonal injection in great measure replicate the pattern of the central projections of the whole ampullary nerve. Because second-order neurons innervated by single utricular afferents are so diverse in location and, by inference, in their functional connections, several characteristics are suggested. First, there is a great redundancy in the afferent projections. Second, the same type of sensory signal is distributed to different central projection pathways, which undoubtedly include vestibulo-ocular, vestibulo-spinal, commissural, and cerebellar connections.

Vestibular nuclei projections

Early studies of vestibular afferent projections used degeneration and Golgi techniques that made it difficult to catalog the projections of specific portions of the vestibular nerve to the brainstem. With the introduction of neural tracers, such as HRP, this task has become easier. Early studies demonstrated that the primary afferents projected to all areas of the VNC except for the LVe (Walberg et al., 1958; Stein and Carpenter, 1967; Gacek, 1969). Those studies included the MVeMC as part of the LVe, referred to as the ventral LVe, which was seen to receive afferent input. In mammals, investigators have examined projections of all the branches of the vestibular nerve by labeling the whole nerve or injecting tracer into the end organ or into a single unit. In general, these studies demonstrate that projections to the VNC overlap extensively but are not homogeneous.

The MVe receives heavy innervation from all three semicircular canals in the gerbil (Kevetter and Perachio, 1986; Perachio et al., 1988), cat (Mannen et al., 1982; Siegborn and Grant, 1983; Sato et al., 1989; Sato and Sasaki, 1993), squirrel monkey (Naito et al., 1995), guinea pig (Gstoettner et al., 1992), and pigeon (Dickman and Fang, 1996). In contrast, saccular projections to the MVe are sparse in the cat (Imagawa et al., 1998), guinea pig (Gstoettner et al., 1992), and gerbil (Kevetter and Perachio, 1986) and appear primarily in the rostral and caudal poles of the nucleus. In the squirrel monkey, saccular afferents were reported in the rostral and dorsal portions of the nucleus (Naito et al., 1995). Previous studies of utricular nerve found MVe projections to be modest. Siegborn and Grant (1983) found terminals limited to the rostral and lateral portions of the nucleus, whereas other studies in the guinea pig (Gstoettner et al., 1992) and cat (Imagawa et al., 1995) did not investigate the distribution of labeling in this nucleus. The heaviest utricular projections to the MVe in the squirrel monkey (Naito et al., 1995) and pigeon (Dickman and Fang, 1996) were rostral. In the current experiment, both single-unit and whole nerve injections produced the heaviest labeling in the parvicellular, especially rostral, portions of this nucleus; it also produced significant ventral and medial labeling in the caudal half of the nucleus. The MVeMC was less heavily labeled.

The anterior, posterior, and horizontal canals all project to the SuVe in gerbils (Kevetter and Perachio, 1986; Perachio et al., 1988), cats (Sato et al., 1989; Sato and Sasaki, 1993; Seigborn et al., 1991); guinea pigs (Gstoettner et al., 1992), pigeons (Dickman and Fang, 1996), and squirrel monkeys (Naito et al., 1995). No saccular projections to the SuVe were seen in the gerbil (Kevetter and Perachio, 1986), whereas single saccular units in the cat collateralize into the caudal/lateral portion of this nucleus (Imagawa et al., 1998). Placement of HRP crystals on the saccular nerve causes sparse labeling of the lateral SuVe nucleus in the guinea pig (Gstoettner et al., 1992); in

contrast, utricular nerve afferents project most heavily to the inferior part of the nucleus. Little input to the SuVe was seen in the cat after labeling either the whole utricular nerve (Siegborn and Grant, 1983) or individual fibers (labeling was confined to the ventrocaudal SuVe; Imagawa et al., 1995). In the squirrel monkey, utricular nerve labeling in the SuVe was seen primarily in dorsolateral areas (Naito et al., 1995). In the present study, ascending fibers were seen particularly in the lateral portion of this nucleus, and terminals were noted in the lateral portion of the nucleus as well. The more medial portions, including the central portion with larger cells, had far fewer fibers and terminals. The rostral cap of the nucleus was also labeled.

Review of the literature concerning afferent projections to the ventral LVe must be done with caution. Early studies make no distinction between the ventral LVe and what we refer to as the MVeMC (Rubertone et al., 1995). Our data also failed to demonstrate utricular innervation of the dorsal LVe, although some labeling appeared in the ventral LVe at the interface between the LVe and MVeMC. In this region, the distinction between the LVe and MVeMC is not always clear, and the neurons in this region that receive canal and/or otolith input may be functionally distinct from the main portion of the LVe. Projections to the ventral LVe have been found from afferents of all three semicircular canals, the sacculus, and the utricle in cats (Mannen et al., 1982; Siegborn and Grant, 1983; Sato et al., 1989; Sato and Sasaki, 1993; Imagawa et al., 1995), guinea pigs (Gstoettner et al., 1992), and gerbils (Kevetter and Perachio, 1986; Perachio et al., 1988). The lateral portion of the nucleus receives saccular projections in the gerbil (Kevetter and Perachio, 1986), guinea pig (Gstoettner et al., 1992), and cat (Imagawa et al., 1998). Previous studies have not definitely demonstrated that the dorsal portion of the LVe receives significant primary afferent innervation.

The SpVe is innervated by afferents from the utricle, saccule, and all three canals. Our results on utricular projections to this nucleus are consistent with those in the literature (Gstoettner et al., 1992; Imagawa et al., 1995; Naito et al., 1995), although our study shows weaker projections to the SpVe than those to the SuVe and MVePC.

Nucleus Y has conflicting nomenclature associated with it. In the mouse, Fredrickson and Trune (1986) clearly distinguish between Y and Inf. This nomenclature is consistent with Paxinos and Watson (1998) and is therefore followed in this paper as well. In the rat, Rubertone et al. (1995) consider Y to be contiguous with group L (first described in the cat by Brodal and Pompeiano [1957]). As in the rat (Rubertone et al., 1995), the caudal end of SuVe, group L, and the ventral nucleus Y are difficult to separate with precision in the gerbil. Rubertone et al. (1995) therefore recommend that L and Y be described as Y in the rat. In the gerbil, a tight cluster of cell bodies caps the inferior cerebellar peduncle that corresponds to Y (Kevetter and Perachio, 1986). Utricular macula injections clearly labeled this area in the current study, although the projection is not as strong as seen from the saccule (Kevetter and Perachio, 1986). Similarly, the region of the Inf (or dorsal Y after Highstein and Reisine [1979]) also has labeling throughout, although it is less dense. In the past, primary afferent inputs to this nucleus have not been documented, although primary vestibular projections to the ventral aspect of the dentate nucleus noted in degeneration studies may correspond to this projection (Brodal and Høivik, 1964).

Saccular input to Y is reported in the mouse (Fredrickson and Trune, 1986), gerbil (Kevetter and Perachio, 1986), cat (Gacek, 1969), and guinea pig (Gstoettner et al., 1992), although a study that intracellularly labeled single saccular afferents in the cat (Imagawa et al., 1998), found none that terminated in nucleus Y. One report demonstrated horizontal canal afferent projections to nucleus Y (Sato et al., 1989), but other studies have not demonstrated canal innervation of this nucleus (Mannen et al., 1982; Gstoettner et al., 1992). In squirrel monkeys, Naito et al. (1995) did not see a projection to Y from the utricle, nor was this connection seen in the guinea pig (Gstoettner et al., 1992). The same BDA technique described in this report (Newlands et al., 2001) has demonstrated utricular and saccular projections to Y in macaques.

The interstitial nucleus of the vestibular nerve receives collaterals from canal and otolith afferents (Mannen et al., 1982; Perachio et al., 1988; Sato et al., 1989; Naito et al., 1995). The current study demonstrates utricular input to this nucleus. The interstitial nucleus is known to project to the flocculus (Langer et al., 1985) and also to receive input from collaterals of the vestibular efferents in gerbils (Shinder et al., 2001) although the function of the nucleus remains obscure.

Extravestibular brainstem projections

Korte (1979) identified discrete terminals lateral to the abducens nuclei and in the rostral ECu by using silver impregnation techniques after whole nerve cuts in cats. Autoradiographic studies showed labeling in the ECu, the subtrigeminal lateral reticular nucleus, perihypoglossal nuclei, and rostral dorsal portions of the nucleus reticularis gigantocellularis (Carleton and Carpenter, 1984). In the chinchilla, HRP labeling shows afferent projections to the parvicellular reticular formation ventromedial to the LVe (Newman et al., 1992).

The areas of the brainstem that Lorente de No (1933) considered to receive vestibular afferent input from the utricle include the ECu, the lateral reticular formation, and the nucleus gigantocellularis. In the gerbil, all these receive saccular afferents (Kevetter and Perachio, 1986). In the cat (Imagawa et al., 1998), a limited sample of intracellularly labeled saccular neurons showed projection to the parvicellular region of the spinal trigeminal nucleus and the reticular formation near both the trigeminal nucleus and the abducens nucleus. Siegborn and Grant (1983) found no terminal labeling outside the major vestibular nuclei after applying HRP to the cut end of the utricular nerve in the cat. In the current study, extravestibular labeling in the brainstem was present but was sparse in the DMGi, nucleus of Roller, and ECu.

After labeling the utricular nerve with HRP crystals applied to the cut nerve, Imagawa et al. (1995) noted thick, labeled axons in the ipsilateral abducens nucleus. There were no labeled terminals. Despite physiologic evidence of utricular nerve input into the abducens nucleus presented in that study, anatomic evidence of this connection is controversial. In the current study, we did not see terminals in the abducens nucleus with either whole nerve or single-unit intracellular fills. It is unlikely that this is due to incomplete filling because our filled units projected to more distant targets, including the ECu and

the cerebellar cortex. With the macular injections, labeled efferent fibers coursed through and near this nucleus. Other authors have also failed to identify projections to the abducens with various modes of vestibular nerve labeling (Siegborn and Grant, 1983; Carleton and Carpenter, 1984; Kevetter and Perachio, 1986; Gerrits et al., 1989; Seigborn et al., 1991; Gstoettner et al., 1992; Newman et al., 1992; Imagawa et al., 1995). One autoradiographic study that used tritiated proline and fucose injected into the vestibular ganglion supported this projection (Lang and Kubik, 1979); however, this may be a result of transneuronal transport (Carleton and Carpenter, 1984; Carpenter and Cowie, 1985).

Cerebellar projections

The projection of the vestibular nerve to the cerebellum has been studied using a variety of techniques in a number of different species. Whole nerve degeneration studies reported evidence of primary afferent terminals in the uvula (lobule IX), nodulus (lobule X), and flocculus in the cat (Brodal and Høivik, 1964; Korte and Mugnaini, 1979) and monkey (Carpenter et al., 1972). In the cat, Brodal and Høivik (1964) also found degenerated fibers in the ventral and dorsal paraflocculus, the lingula (lobule I), and the small-celled portion of the lateral cerebellar (dentate) nucleus (Lat) ipsilaterally. Korte and Mugnaini (1979) found the floccular projection to be smaller than the uvula and nodulus projections. Using retrograde HRP labeling of Scarpa's ganglion after injections into the cerebellum, Kotchabhakdi and Walberg (1978) refuted the existence of projections to Lat but suggested that the entire vermis was a target of vestibular primary afferent projections. Carleton and Carpenter (1984) observed projections to the uvula, nodulus, deep folia of vermal lobules V and VI, lingula, and flocculus following peripheral injection of tritiated amino acids in the monkey.

Barmack et al. (1993), using both orthograde and anterograde labeling techniques in the rabbit, confirmed a weak projection to the flocculus and a strong primary afferent projection to the uvula and nodulus. Gerrits et al. (1989) injected wheat germ agglutinin-HRP into the vestibular ganglion of the rabbit and reported anterograde labeling of primary afferent terminals bilaterally in lobules I–II, ipsilaterally in lobules X and IXd, and in the depth of the main fissures separating lobules II–VI. They found no projection to the flocculus. Neither Gerrits et al. (1989) nor Barmack et al. (1993) reported a paraflocular projection. Langer et al. (1985) in their studies on monkey found no Scarpa's ganglion labeling after injection of HRP into the flocculus, although such labeling was seen in the rat (Blanks et al., 1983) and rabbit (Alley et al., 1975).

Other studies have described the cerebellar projection of individual elements of the vestibular nerve. Projections to the uvula and nodulus were seen with transganglionic transport of HRP injected into the cat horizontal canal nerve but not the utricular nerve (Seigborn and Grant, 1983). In the gerbil, application of HRP into the posterior canal ampulla identified cerebellar labeling in the uvula, nodulus, and some vermal areas more dorsally (Kevetter and Perachio, 1986). Injection into the sacculus produced labeling in the lingula, uvula, and parts of the culmen-declive (lobules III–-IV). No labeling was seen in the flocculus or paraflocculus. Purcell and Perachio (2001) injected HRP into the uvula/nodulus and flocculus in gerbils. They identified retrograde transganglionic labeling of terminals in all five end organs after the vermal injection, but only ampullary afferents labeled after floccular injections.

Our results documenting utricular projections in the gerbil primarily to lobules IX and X, with no projections to the flocculus and paraflocculus, are consistent with previous findings in this species (Purcell and Perachio, 2001). Sparse labeling was present in the deep cerebellar nuclei, particularly boutons en passant in Med and IntP. Although earlier degeneration studies suggested such a projection, vestibular afferent terminations in the cerebellar nuclei had not been demonstrated using HRP (Gerrits et al., 1989).

CONCLUSIONS

Single and multiunit studies using neuronal tracers to delineate the central projections of vestibular afferents add significantly to our understanding of the vestibular system. The morphological features of the central projections of utricular afferents share some of the same characteristics reported for canal afferents and thus illustrate some of the commonalities shared across the various divisions of the vestibular nerve. However, processing of vestibular signals beyond the first synapse shapes the output of the system. Clearly, understanding the distribution and utilization of utricular inputs to the central nervous system will involve deeper understanding of the polysynaptic pathways.

ACKNOWLEDGMENTS

We thank Sid Stephans and Heather McMullen for technical assistance. We also thank Dr. Galen Kaufman for use of his "gerbil atlas" for Figure 4.

LITERATURE CITED

Alley K, Baker R, Simpson JI. 1975. Afferents to the vestibulo-cerebellum and the origin of the visual climbing fibers in the rabbit. Brain Res 98:582–589.

Angelaki DE, Dickman JD. 2000. Spatiotemporal processing of linear acceleration: primary afferent and central vestibular neuron responses. J Neurophysiol 84:2113–2132.

Angelaki DE, McHenry MQ, Dickman JD, Newlands SD, Hess BJM. 1999. Computation of inertial motion: neural strategies to resolve ambiguous otolith information. J Neurosci 19:316–327.

Barmack NH, Baughman RW, Errico P, Shojaku H. 1993. Vestibular primary afferent projection to the cerebellum of the rabbit. J Comp Neurol 327:521–534.

Blanks RHI, Precht W, Torigoe Y. 1983. Afferent projections to the cerebellar flocculus in the pigmented rat demonstrated by retrograde transport of horseradish peroxidase. Exp Brain Res 52:293–306.

Brodal A, Høivik B. 1964. Site and mode of termination of primary vestibulocerebellar fibres in the cat. Arch Ital Biol 102:1–21.

Brodal A, Pompeiano O. 1957. The vestibular nuclei in the cat. J Anat 91:438–454.

Burian M, Gstoettner W, Mayr R. 1990. Brainstem projection of the vestibular nerve in the guinea pig: an HRP (horseradish peroxidase) and WGA-HRP (wheat germ agglutinin-HRP) study. J Comp Neurol 293: 166–177.

Carleton SC, Carpenter MB. 1984. Distribution of primary vestibular fibers in the brainstem and cerebellum of the monkey. Brain Res 294:281–298.

Carpenter MB, Cowie RJ. 1985. Transneuronal transport in the vestibular and auditory systems of the squirrel monkey and the arctic ground squirrel. I. Vestibular system. Brain Res 358:249–263.

Carpenter MB, Stein BM, Peter P. 1972. Primary vestibulocerebellar fibers

in the monkey: distribution of fibers arising from distinctive cell groups of the vestibular ganglia. Am J Anat 135:221–249.

Dickman JD, Fang Q. 1996. Differential central projections of vestibular afferents in pigeons. J Comp Neurol 367:110–131.

Didier A, Cazals Y, Aurousseau C. 1987. Brainstem connections of the anterior and posterior parts of the saccule in the guinea pig. Acta Otolaryngol (Stockh) 104:385–391.

Fernández C, Goldberg JM, Baird RA. 1990. The vestibular nerve of the chinchilla. III. Peripheral innervation patterns in the utricular macula. J Neurophysiol 63:767–780.

Fredrickson CJ, Trune DR. 1986. Cytoarchitecture and saccular innervation of nucleus y in the mouse. J Comp Neurol 252:302–322.

Gacek RR. 1969. The course and central termination of first order neurons supplying vestibular endorgans in the cat. Acta Otolaryngol Suppl 254:1–66.

Gacek RR. 1977. Location of brain stem neurons projecting to the oculomotor nucleus in the cat. Exp Neurol 57:725–749.

Gerrits NM, Epema AH, Van Linge A, Dalm E. 1989. The primary vestibulocerebellar projection in the rabbit: absence of primary afferents in the flocculus. Neurosci Lett 105:27–33.

Goldberg JM, Desmadryl G, Baird RA, Fernández C. 1990. The vestibular nerve of the chinchilla IV. Discharge properties of utricular afferents. J Neurophysiol 63:781–790.

Gstoettner W, Burian M, Cartellieri M. 1992. Central projections from singular parts of the vestibular labyrinth in the guinea pig. Acta Otolaryngol 112:486–495.

Highstein SM, Reisine H. 1979. Synaptic and functional organization of vestibulo-ocular reflex pathways. In: Granit R, Pompeiano O, editors. Reflex control of posture and movement. Prog Brain Res 50:431–442.

Imagawa M, Isu N, Sasaki M, Endo K, Ikegami H, Uchino Y. 1995. Axonal projections of utricular afferents to the vestibular nuclei and the abducens nucleus in cats. Neurosci Lett 186:87–90.

Imagawa M, Graf W, Sato H, Suwa H, Isu N, Izumi R, Uchino Y. 1998. Morphology of single afferents of the saccular macula in cats. Neurosci Lett 240:127–130.

Kevetter GA, Perachio AA. 1986. Distribution of vestibular afferents that innervate the sacculus and posterior canal in the gerbil. J Comp Neurol 254:410–424.

Kiang NY, Rho JM, Northrop CC, Liberman MC, Ryugo DK. 1982. Hair-cell innervation by spinal ganglion cells in adult cats. Science 217:175–177.

Korte GE. 1979. The brainstem projection of the vestibular nerve in the cat. J Comp Neurol 184:279–292.

Korte GE, Mugnaini E. 1979. The cerebellar projection of the vestibular nerve in the cat. J Comp Neurol 184:265–278.

Kotchabhakdi N, Walberg F. 1978. Primary vestibular afferent projections to the cerebellum as demonstrated by retrograde axonal transport of horseradish peroxidase. Brain Res 142:142–146.

Lang W, Kubik, S. 1979. Primary vestibular afferent projections to the ipsilateral abducens nucleus in cats. An autoradiographic study. Exp Brain Res 37:177–181.

Langer T, Fuchs AF, Scudder CA, Chubb MC. 1985. Afferents to the flocculus of the cerebellum in the Rhesus macaque as revealed by retrograde transport of horseradish peroxidase. J Comp Neurol 235:1–25.

Lee WS, Newman A, Honrubia V. 1992. Afferent innervation of the vestibular nuclei in the chinchilla. I. A method for labeling individual vestibular receptors with horseradish peroxidase. Brain Res 597:269–277.

Lorente de No R. 1933. Anatomy of the eighth nerve. The central projections of the nerve endings of the internal ear. Laryngoscope 43:1–38.

Mannen H, Sasaki S, Ishizuka N. 1982. Trajectory of primary vestibular fibers originating from the lateral, anterior, and posterior semicircular canals in the cat. Proc Jpn Acad 58:237–242.

Merfield DM, Zupan L, Peterka RJ. 1999. Humans use internal models to estimate gravity and linear acceleration. Nature 398:615–618.

Naito Y, Newman A, Lee WS, Beykirch K, Honrubia V. 1995. Projections of the individual vestibular end-organs in the brain stem of the squirrel monkey. Hearing Res 87:141–156.

Newlands SD, Vrabec JT, Purcell IM, Stewart CM, Zimmerman B, Perachio AA. 2001. Central projections of the utricular and saccular nerves in the macaque. Soc Neurosci Abstr 27:#298.13.

Newman A, Suarez C, Lee WS, Honrubia V. 1992. Afferent innervation of the vestibular nuclei in the chinchilla. II. Description of the vestibular nerve and nuclei. Brain Res 597:278–297.

Paxinos G, Watson C. 1998. The rat brain in stereotaxic coordinates. San Diego: Academic Press.

Perachio AA, Correia MJ. 1983. Responses of semicircular canal and otolith afferents to small angle static head tilts in the gerbil. Brain Res 280:287–298.

Perachio AA, Kevetter GA. 1986a. Cerebellar cortical and nuclear projections of untricular afferents in the gerbil. Neurosci Abstr 12:254.

Perachio AA, Kevetter GA. 1986b. Physiological and anatomical characteristics of HRP-filled otolith afferents in the gerbil. In: Proceedings of the ASGSB Meeting, 1986.

Perachio AA, Kevetter GA. 1989. Identification of vestibular efferent neurons in the gerbil: histochemical and retrograde labelling. Exp Brain Res 78:315–326.

Perachio AA, Kevetter GA, Corriea MJ. 1984. Projections of individual otolith primary afferents in the gerbil. Neurosci Abstr 10:1153.

Perachio AA, Dickman JD, Corriea MJ. 1988. Morphological and functional characteristics of semicircular canal afferents sensitive to head tilt. In: Hwang JC, Daunton NG, Wilson VJ, editors. Basic and applied aspects of vestibular function. Hong Kong: Hong Kong University Press. p 13–25.

Purcell IM, Perachio AA. 1997. Three-dimensional analysis of vestibular efferent neurons innervating semicircular canals of the gerbil. J Neurophysiol 78:3234–3248.

Purcell IM, Perachio AA. 2001. Peripheral patterns of terminal innervation of vestibular primary afferent neurons projecting to the vestibulocerebellum in the gerbil. J Comp Neurol 432:48–61.

Rubertone JA, Mehler WR, Voogd J. 1995. The vestibular nuclear complex. In: Paxinos G, editor. The rat nervous system. San Diego: Academic Press. p 773–796.

Saper CD. 1999. Image is everything. J Comp Neurol 412:381–382.

Sato F, Sasaki H. 1993. Morphological correlations between spontaneously discharging primary vestibular afferents and vestibular nucleus neurons in the cat. J Comp Neurol 333:554–566.

Sato F, Sasaki H, Ishizuka N, Sasaki S, Mannen H. 1989. Morphology of single primary vestibular afferents originating from the horizontal semicircular canal in the cat. J Comp Neurol 290:423–439.

Shinder ME, Purcell IM, Kaufman GD, Perachio AA. 2001. Vestibular efferent neurons project to the flocculus. Brain Res 889:288–294.

Siegborn J, Grant G. 1983. Brainstem projections of different branches of the vestibular nerve. An experimental study by transganglionic transport of horseradish peroxidase in the cat I. The horizontal ampullar and utricular nerves. Arch Ital Biol 121:237–248.

Siegborn J, Yingcharoen K, Grant G. 1991. Brainstem projections of different branches of the vestibular nerve: an experimental study by transganglionic of horseradish peroxidase in the cat. Anat Embryol 184:291–299.

Stein BM, Carpenter MB. 1967. Central projections of portions of vestibular ganglia innervating specific parts of the labyrinth in the rhesus monkey. Am J Anat 120:281–318.

Veenman CL, Reiner A, Honig MG. 1992. Biotinylated dextran amine as an anterograde tracer for single- and double-labeling studies. J Neurosci Methods 41:239–254.

Walberg F, Bowsher D, Brodal A. 1958. The termination of primary vestibular fibers in the vestibular nuclei in the cat. An experimental study with silver methods. J Comp Neurol 110:391–419.